JOURNAL OF Applied Polymer SCIENCE

# Tuning the photovoltaic performances of the terpolymers based on thiophene-benzene-thiophene via the modification of alkyl side chains

**Huan Guo, Tianpei Shen, Fen Wu, Rongyan Hou, Xuxu Liu, Bin Zhao, Songting Tan**
College of Chemistry and Key Laboratory of Polymer Applied Technology of Hunan Province, Xiangtan University, Xiangtan 411105, People's Republic of China
Correspondence to: S. Tan (E-mail: tanst2008@163.com)

**ABSTRACT:** Three new random conjugated terpolymers based on thiophene-2,5-bis((2- ethylhexyl)oxy)benzene-thiophene or thiophene-2,5-bis((2-octyl)oxy)benzene- thiophene as electron-donating units, diketopyrrolopyrrole (DPP) and 4,7-dithien-5-yl-2,1,3-benzothiadiazole (DTBT) side group as electron-withdrawing units have been designed and synthesized by Stille-coupling reaction. All the terpolymers exhibit good thermal stability, broad absorption in the range of 300 to 800 nm. By tuning the alkyl side chains of the terpolymers, the absorption spectra, HOMO energy levels and photovoltaic properties of the terpolymers changed dramatically. A bulk heterojunction polymer solar cell fabricated from terpolymer **GP2** and $PC_{61}BM$ exhibited a promising power conversion efficiency of 3.31% without any processing additives. © 2015 Wiley Periodicals, Inc. J. Appl. Polym. Sci. **2016**, *133*, 42982.

**KEYWORDS:** functionalization of polymers; properties and characterization; synthesis and processing

Received 1 June 2015; accepted 25 September 2015
**DOI: 10.1002/app.42982**

## INTRODUCTION

Bulk heterojunction (BHJ) polymer solar cells (PSCs) have been intensively studied in recent years for their low-cost, roll-to-roll production and environment friendly. Over the past decade, many studies have been done in this field, so the power conversion efficiency (PCE) of BHJ PSCs has improved significantly and that of single-junction BHJ PSCs have gradually exceeded 10%.[1,2] Although progress has been impressive, the efficiencies of PSCs are still not satisfactory when compared with the inorganic counterparts.[3] In order to improve the performance of the PSCs, further improvements in many factors are in urgent need.[4–11]

It is well recognized that polymers require a broad and strong absorption in the visible to near-infrared region as well as possible to achieve a high photovoltaic performance.[12] To obtain the broad and strong absorption, design and synthetize the low band-gap conjugated polymers is a strategy we frequently used. Generally, most random conjugated polymers exhibit two distinguishing absorption, a main absorption above 600 nm and a weak absorption between 400 and 600 nm. The former is owe to the strong intramolecular charge transfer (ICT) that occurs between donor and acceptor, the latter is attributed to the localized $\pi-\pi^*$ transition of the polymer backbone.[13,14] In the past few years, a promising approach was to develop random terpolymers by copolymerizing one electron-rich unit and two different electron-deficient units or one electron-deficient unit and two different electron-rich units to broaden the absorption spectrum.[15–18]

For binary and terpolymers, the alkyl side chains are crucial for solubility and processability. Although long or bulky aliphatic groups can make sure a good solubility of the polymers in common organic solvent; however, this can bring negative impact on other factors such as packing, blend morphology, and fullerene miscibility.[19] So optimizing the alkyl side chains to balance the crystallinity, and solubility is requisite for high performance PSCs.

Here, we designed and synthesized a new series of random conjugated terpolymers (**GP1**, **GP2,** and **GP3**, Figure 1), by using diketopyrrolopyrrole (DPP) and 4,7-dithien-5-yl-2,1,3-benzothiadiazole (DTBT) as the electron-deficient unit (A), alternating with electron-rich thiophene-2,5-bis((2-alkyl)oxy)benzene-thiophene segments in a regular fashion. The absorption spectrum of the polymer containing DPP unit can expand to near-infrared from visible region because of its electron-deficient lactam rings and strong $\pi-\pi$ interactions.[20] It has been copolymerized with several different electron-rich units,[21–28] such as benzo(1,2-*b*:4,5-*b*′)dithiophene (BDT) and thienylbenzodithiophene (BDTT), providing polymers with excellent performance in photovoltaic cells. The 4,7-dithien-5-yl-2,1,3-benzodiathiazole (DTBT) side groups is an effective electron-deficient unit, but the polymer based on DTBT possesses relatively narrow absorption spectrum and low hole mobility.[29] By combining the DPP

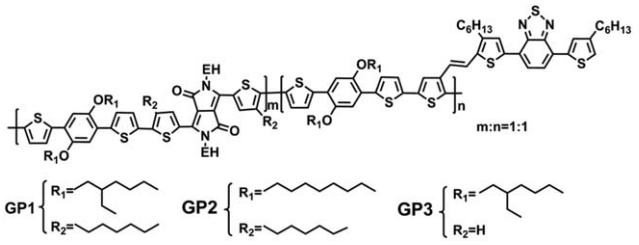


**Figure 1.** The chemical structure of the terpolymers.

unit and DTBT side groups, the terpolymers would achieve broad absorption spectra and excellent photoelectrical performances. The thiophene-benzene-thiophene unit is a relatively tortile conjugated block because of steric hindrance, which would lead to a deep HOMO energy level and a high $V_{oc}$.[30–32] So we introduced the thiophene-2,5-bis((2-alkyloxy)benzene-thiophene (TBT) with the linear and branched alkyloxy side-chain as electron-rich unit. The effects of the different alkyloxy side groups on the thermal, photophysical, electrochemical and photovoltaic properties of the terpolymers were investigated in detail, and we acquired the power conversion efficiency (PCE) of 1.41%, 3.31% and 3.05% based on the side chain conjugated terpolymers **GP1**, **GP2,** and **GP3**, respectively.

## EXPERIMENTAL

### Materials and Chemicals

3,6-Bis(5-bromothiophen-2-yl)-2,5-bis(2-ethylhexyl)-2,5-dihydropyrrolo[3,4-*c*]pyrrole-1,4-dione (**M2**) was purchased from Derthon Optoelectronic Materials Science Technology Co. Ltd (Shenzhen, China) and were used without further purification. *n*-BuLi, $Pd(PPh_3)_4$, $(C_4H_9)_3SnCl$ and chlorobenzene (CB) were obtained from Alfa Aesar and used as received. Other reagents and solvents were purchased commercially as analytical-grade quality and used without further purification. Tetrahydrofuran (THF) and toluene was dried over Na/benzophenone and freshly distilled prior to use. 4-Hexylthiophene-2-carbonitrile (**1**),[33] 1,4-dibromo-2,5-bis((2-octyl)oxy)benzene (**4**),[34] 1,4-bis(2-(5-trimethylstannyl)thienyl)-2,5-bis(2-ethylhexyloxy)benzene (**M4**),[30] (E)-5-(7-(5-(2-(2,5-dibromothiophen-3-yl)vinyl)-4-hexylthiophen-2-yl)benzo[1,2,5]thiadiazol-4-yl)-3-hexylthiophene-2-carbaldehyde (**M5**)[29] were synthesized according to literature procedures.

### Characterization

Nuclear magnetic resonance (NMR) spectra were measured with Bruker AVANCE 400 spectrometer. MALDI-TOF mass spectrometric measurements were performed on Bruker Autoflex III. UV-Visible-Near Infrared (UV-Vis-NIR) absorption spectra of the polymers were conducted on a Perkin-Elmer Cary 100 UV-Vis-NIR spectrometer. The average molecular weight and polydispersity index (PDI) of the polymers were determined using Waters 1515 gel permeation chromatography (GPC) analysis with THF as eluent and polystyrene as standard. Thermogravimetric analysis (TGA) measurement was conducted on a Netzsch TG 209 analyzer under nitrogen at a heating rate of 20°C $min^{-1}$. Electrochemical redox potentials were obtained by cyclic voltammetry (CV) using a three-electrode configuration and an electrochemistry workstation (ZAHNER ZENNIUM) at a scan rate of 100 mV $s^{-1}$. CV was conducted with the thin film on a Pt plate as the working electrode, Pt slice as the counter electrode, and Ag/AgCl (Ag in a 0.01 mol/L KCl) electrode as the reference electrode. The supporting electrolyte is 0.1 M *tetra-n*-butylammonium hexafluorophosphate ($Bu_4NPF_6$) in anhydrous acetonitrile solution. Atomic force microscopy (AFM) measurements were measured with Veeco Multimode 8 in a tapping mode.

### Synthetic Routes for Monomers and Polymers

**3,6-Bis(4-hexylthiophen-2-yl)2,5-Dihydropyrrolo[3,4-C] pyrrole-1,4-Dione (2).** Firstly, potassium tert-butoxide (5.40 g, 48.12 mmol) and t-amyl alcohol (80 mL) was added to a two-necked 250 mL round-bottom flask with argon protection. Then 4-hexylthiophene-2-carbonitrile (**1**) (8.00 g, 41.38 mmol) was dropped by a syringe one portion. The mixture was warmed up to 110°C, and a solution of dimethyl succinate (2.71 mL, 20.69 mmol) in t-amyl alcohol (8 mL) was added dropwise. The reaction mixture was kept at 110°C for 7 h. When the mixture was cooled to room temperature, acetic acid (5.00 mL) was added to neutralized the remainder sodium tert-butylate. Then the mixture was poured into methanol (100 mL) for 1 h. The suspension was filtered, and washed by methanol and water twice each. The red solid was dried and without further purification (3.30 g, 34.0%).

**3,6-Bis(4-hexylthiophen-2-yl)2,5-Diethylhexylpyrrolo[3,4-*c*] pyrrole-1,4-Dione (3).** 3,6-Bis(4-hexylthiophen-2-yl)2,5-dihydropyrrolo[3,4-*c*]pyrrole-1,4-dione (**2**) (2.00 g, 4.27 mmol) and anhydrous potassium carbonate (2.95 g, 21.35 mmol) were added into two-necked 100 mL round-bottom flask. Then *N*, *N*-dimethylformamide (60 mL) was added and heated to 60°C for 1 h, under argon protection. 2-Ethylhexyl bromide (2.39 g, 2.29 mL, 12.90 mmol) was added by a syringe in one portion. After the addition was completed, the reaction mixture was stirred for 15 h at 125°C. When the mixture was cooled to room temperature, the mixture was partitioned between DCM and water. The organic phase was dried by anhydrous $MgSO_4$, and then the solvent was evaporated under vacuum. The crude product was purified by silica gel chromatography with dichloromethane/petroleum ester (1:1 by volume) as eluents, giving a purple-black solid (1.50 g, 50.7%). $^1$H-NMR (400 MHz, $CDCl_3$, $\delta$/ppm): 8.72 (s, 2H), 7.23 (s, 2H), 4.01–3.87 (d, 4H), 2.72–2.68 (t, 4H), 1.87 (s, 2H), 1.87–1.68 (t, 4H), 1.35–1.24 (m, 28H), 0.89–0.85 (m, 18H). MALDI-TOF MS ($C_{42}H_{64}N_2O_2S_2$) m/z: calcd for 692.441, found 692.499.

**3,6-Bis(5-bromo-4-hexylthiophen-2-yl)-2,5-Bis(2-ethylhexyl) Pyrrolo[3,4-C]pyrrole-1,4-Dione (M1).** 3,6-Bis(4-hexylthiophen-2-yl)−2,5-diethylhexylpyrrolo[3,4-*c*]pyrrole-1,4-dione (**3**) (1.00 g, 1.44 mmol) was dissolved in $CHCl_3$ (30 ml) and stirred at 0°C. Protected from light, NBS (0.51 g, 2.88 mmol) in $CHCl_3$ (10 mL) was added to the mixture and kept at 0°C for 2 h. The mixture was partitioned between DCM and water. The organic phase was dried by anhydrous $MgSO_4$, and then the solvent was evaporated under vacuum. The residue was purified by column chromatography on a silica gel (petroleum ester/$CH_2Cl_2$ = 4:1, v:v) to afford the title compound as a purple solid (0.60 mg, 49.0%). $^1$H NMR (400 MHz, $CDCl_3$, $\delta$/ppm): 8.57 (s, 2H), 3.94–3.92 (d, 4H), 2.66–2.63 (t, 4H), 1.84 (s, 2H),

1.66-1.64 (t, 4H), 1.33-1.25 (m, 28H), 0.88–0.86 (m, 18H). $^{13}$C NMR (100 MHz, $CDCl_3$, $\delta$/ppm): 161.41, 143.95, 139.33, 135.57, 129.35, 116.18, 107.91, 45.99, 39.13, 31.59, 30.24, 29.61, 29.48, 28.95, 28.37, 23.70, 23.06, 22.61, 14.05, 13.98, 10.58. MALDI-TOF MS ($C_{42}H_{64}N_2O_2S_2$) m/z: calcd for 848.262, found 848.290.

**1,4-Bis(2-thienyl)-2,5-Bis((2-octyl)oxy)Benzene (5).** 1,4-Dibromo-2,5-bis((2-octyl)oxy)benzene **(4)** (2.00 g, 4.06 mmol), 2-(tributylstannyl)thiophene (4.84 g, 12.99 mmol), and tetrakis(triphenylphosphine) palladium ($Pd(PPh_3)_4$) (0.24 g) were introduced into a round-bottomed flask (100 mL) with 50 mL toluene under a nitrogen atmosphere. The solution was stirred at 110°C for 48 h, then toluene was removed, and a solution of ammonium fluoride (100 mL) in water and $CH_2Cl_2$ (120 mL) were added. The mixture was stirred vigorously for 2 h, then extracted with $CH_2Cl_2$ (3 × 50 mL). The organic layer was washed with a saturated aqueous solution of sodiumchloride (50 mL). After drying over anhydrous sodium sulfate, it was concentrated and the crude product was purified by silica gel column chromatography using petroleum ether/$CH_2Cl_2$ (10:1, v:v) as eluent to give compound (**5**) as a sticky liquid in 74.1% yield (1.50 g). $^1$H-NMR (400 MHz, $CDCl_3$, $\delta$/ppm): 7.54–7.53 (d, 2H), 7.34–7.33 (d, 2H), 7.26 (s, 2H), 7.10–7.09 (t, 2H), 4.10–4.06 (t, 4H), 1.93–1.87 (m, 4H), 1.53–1.51 (m, 4H), 1.35–1.29 (m, 16H), 0.90–0.87 (t, 6H). $^{13}$C NMR (100 MHz, $CDCl_3$, $\delta$/ppm): 149.26, 139.34, 126.76, 125.71, 125.19, 122.97, 112.80, 69.75, 31.88, 29.47, 29.42, 29.29, 26.28, 22.74, 14.20. MALDI-TOF MS ($C_{30}H_{42}O_2S_2$) m/z: calcd for 498.783; found 498.343.

**1,4-Bis(2-(5-trimethylstannyl)thienyl)-2,5-Bis((2-octyl)oxy) Benzene (M3).** To a solution of compound **5** (1.50 g, 3.01 mmol) in dry THF (15 mL), a solution of *n*-butyllithium in petroleum ether (3.60 mL, 2.5*M*) was added dropwise at −78°C under argon atmosphere. The mixture was stirred for 30 min at −78°C, then the resulting solution was warmed to room temperature and stirred for another 1 h. The mixture was cooled to −78°C again, and trimethyltin chloride (1.80 g, 9.03 mmol) in dry THF was added to the mixture. The mixture was stirred at −78°C for 1 h and then stirred at room temperature overnight. The resulting mixture was poured into 50 mL water and 100 mL of petroleum ether. The organic layer was washed twice with 50 mL water and dried over anhydrous $MgSO_4$. The organic layer was evaporated dried over vacuum to afford green solid. The solid was then purified by recrystallization from ethanol to give light green crystals (1.10 g, 66.7% yield). $^1$HNMR (400 MHz, $CDCl_3$, $\delta$/ppm): 7.66–7.65 (d, 2H), 7.24 (s, 2H), 7.18–7.17 (d, 2H), 4.09–4.05 (t, 4H), 1.90–1.84 (m, 4H), 1.54–1.26 (m, 20H), 0.89–0.87 (t, 6H), 0.46–0.32 (m, 18H). $^{13}$C NMR (100 MHz, $CDCl_3$, $\delta$/ppm): 149.24, 145.41, 137.89, 135.10, 126.61, 123.03, 113.09, 69.69, 31.90, 29.54, 29.51, 29.33, 26.41, 22.72, 14.15, −8.25.

**Polymerization for GP1. M1** (52 mg, 0.06 mmol), **M4** (100 mg, 0.12 mmol), and **M5** (45 mg, 0.06 mmol) were dissolved into 8 mL of toluene in a 25 mL flask under argon protection. The solution was flushed with argon for 30 min, and then 10 mg of $Pd(PPh_3)_4$ was added into the flask. The solution was flushed with argon for 30 min again and then it was stirred at 100°C for 72 h under argon atmosphere. After it cooled to room temperature, the mixture was added to methanol, and the precipitated solid was collected and purified by Soxhlet extraction with methanol, acetone, petroleum ether, and chloroform in sequence. The title polymer was obtained as a dark green solid (105 mg, yield 76.9%). $^1$H-NMR (400 MHz, $CDCl_3$, $\delta$/ppm): 8.88 (br), 8.07-6.88 (br), 4.06 (br), 2.95–2.40 (br), 1.92–1.26 (br), 1.01–0.90 (br). Number-average molecular weights ($\overline{M_n}$) = 23 kg/mol, PDI = 1.56.

**Polymerization for GP2. GP2** was prepared using the similar procedure as **GP1** with the monomer **M1** (52 mg, 0.06 mmol), **M3** (100 mg, 0.12 mmol) and **M5** (45 mg, 0.06 mmol). The final product was obtained as a dark blue solid (98 mg, 72%). $^1$H-NMR (400 MHz, $CDCl_3$, $\delta$/ppm): 8.88 (br), 8.02–7.15 (br), 4.13 (br), 2.94–2.68 (br), 1.96–1.31 (br), 0.90 (br). $\overline{M_n}$ = 17 kg/mol, PDI = 1.33.

**Polymerization for GP3.** By following the similar method used for **GP1**, **GP3** was synthesized with the monomer **M2** (50 mg, 0.08 mmol), **M4** (120 mg, 0.15 mmol) and **M5** (53 mg, 0.08 mmol). The polymer was obtained as a dark green solid (115 mg, 75.3%). $^1$H-NMR (400 MHz, $CDCl_3$, $\delta$/ppm): 9.00 (br), 8.00–6.73 (br), 4.02 (br), 2.79–2.51 (br), 1.92–1.25 (br), 0.92 (br). $\overline{M_n}$ = 11 kg/mol, PDI = 1.62.

### Fabrication and Characterization of PSCs

The structure of the solar cells was indium tin oxide (ITO)/$MoO_3$(20 nm)/polymer:$PC_{61}BM$(∼100 nm)/LiF(0.5 nm)/Al(100 nm). The PSC devices were fabricated with ITO glass as a positive electrode and LiF/Al as a negative electrode. The ITO glass was precleaned and then modified by a thin layer of $MoO_3$, which was deposited on ITO surface by vacuum evaporation under 5 × $10^{-4}$ Pa. The photoactive layer was prepared by spin-coating a blend solution of polymer and $PC_{61}BM$ in CB on the surface of ITO/$MoO_3$ substrate. Then, the LiF/Al cathode was deposited on the polymer layer by vacuum evaporation under 5 × $10^{-4}$ Pa. The accurate area of every device is 3.8 $mm^2$, defined by the overlap of the ITO and metal electrode. The current density-voltage (J–V) curves were measured by a Keithley 2602 Source Meter under 100 mW $cm^{-2}$ standard AM 1.5G spectrum using a Sol 3A Oriel solar simulator. The incident light intensity was calibrated using a standard Si solar cell. The measurement of monochromatic incident photon-to-current conversion efficiency (IPCE) was performed using a Zolix Solar Cell Scan 100 QE/IPCE measurement system.

## RESULTS AND DISCUSSION

### Synthesis and Structure Characterization

The synthetic routes for the monomers and the polymers are shown in Scheme 1. Bromination of compound **3** with NBS yielded compound **M1**. Treatment of compound **5** with *n*-BuLi and then trimethyltin chloride gave the monomer **M3**. The structures of the monomers **M1** and **M3** were confirmed by $^1$H NMR, $^{13}$C NMR, and MALDI-TOF MS. The terpolymers were prepared through Stille coupling reactions between the monomer **M3** or **M4** and the bromides (**M1**, **M2,** and **M5**) as shown in Scheme 1. All the polymers exhibited good solubility in common organic solvents, such as chloroform, THF, chlorobenzene,

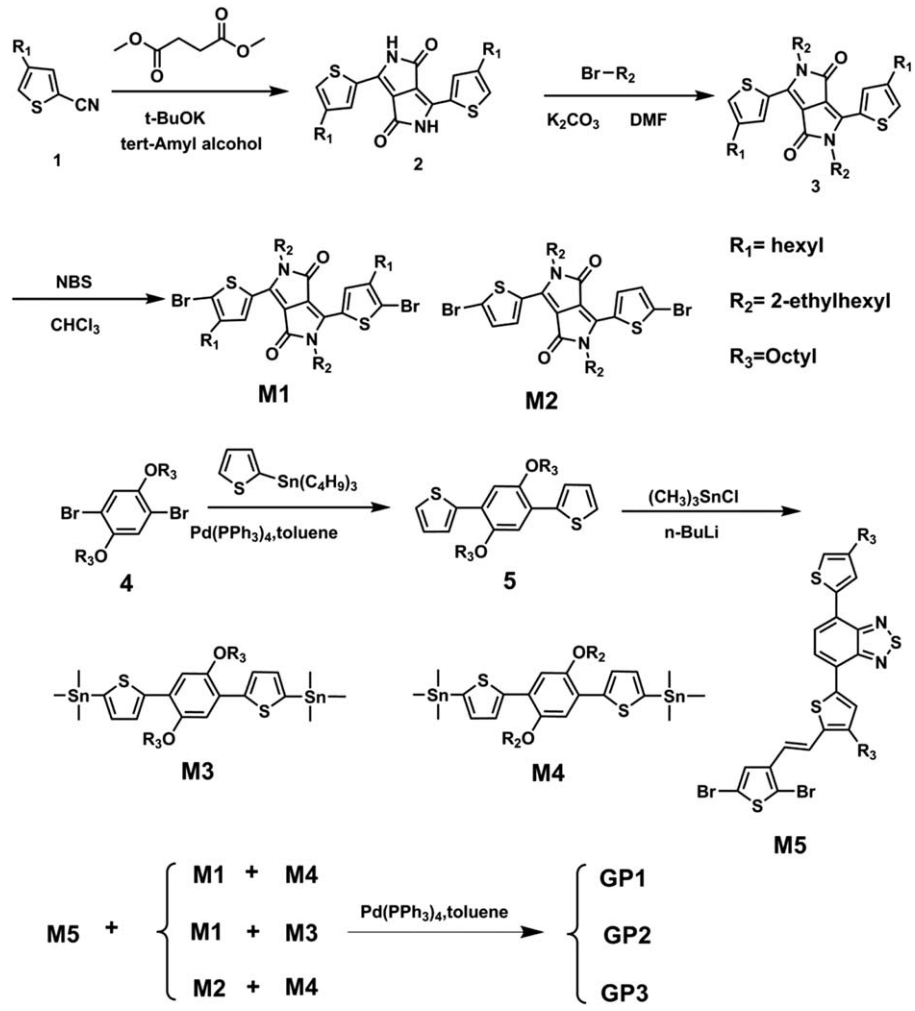


**Scheme 1.** Synthesis of the terpolymers.

and 1,4-dichlorobenzene. The polymerization results and thermal properties of the polymers are summarized in Table I. The number-average molecular weights ($\overline{M_n}$) and polydispersityindexs (PDI), determined by gel permeation chromatography (GPC) using THF as the eluent, are 23 kg mol$^{-1}$ and 1.5 for **GP1**, 17 kg mol$^{-1}$ and 1.3 for **GP2**, 11 kg mol$^{-1}$ and 1.6 for **GP3**, respectively.

### Thermal Properties

The thermal properties of the polymers were investigated by TGA. As shown in Figure 2 and Table I, the TGA curves reveal that the onset temperatures with 5% weight loss ($T_d$) of **GP1**, **GP2,** and **GP3** are 420°C, 399°C, and 401°C, respectively. The $T_d$ of **GP1** is higher relatively than that of **GP2** and **GP3**, because **GP1** possesses higher average molecular weight. And the thermal stability of the three terpolymers is good enough for the applications in optoelectronic devices. However, it did not show any noticeable glass transition in differential scanning calorimetry (DSC) analysis in the temperature range from 40 to 300°C due to conjugated molecules skeleton in main chain.

**Table I.** Molecular Weights and Thermal Properties of the Terpolymers

| Polymers | Yield (%) | $\overline{M_n}$ (kg mol$^{-1}$)[a] | PDI | $T$ (°C)[b] |
|---|---|---|---|---|
| GP1 | 76.9 | 23 | 1.5 | 420 |
| GP2 | 72.0 | 17 | 1.3 | 399 |
| GP3 | 75.3 | 11 | 1.6 | 401 |

[a] Determined by GPC in THF based on polystyrene standards.
[b] Decomposition temperature, determined by TGA in nitrogen, based on 5% weight loss.

### Photophysical Properties

The photophysical properties of the terpolymers are investigated by UV-Vis spectra in diluted $CHCl_3$ solution and thin films on quartz plates. Figure 3 gives the absorption spectra of **GP1**, **GP2,** and **GP3** in diluted $CHCl_3$ solution [Figure 3(a)] and as a thin film [Figure 3(b)], and the correlated data are summarized in Table II. As shown in Figure 3(a), all the terpolymers exhibit two distinct absorption bands. The first absorption bands at shorter wavelengths region (300–550 nm) with the absorption peak wavelength ($\lambda_{s,\ max}$) at 463 nm for **GP1**, 458 nm for **GP2**, 474 nm for **GP3** are attributed to intramolecular charge transfer (ICT) from TBT to DTBT side groups. Obviously, **GP1** and **GP3** have the stronger ICT between TBT and DTBT side groups due to the bulkier but shorter side chain (R = isooctyl). And

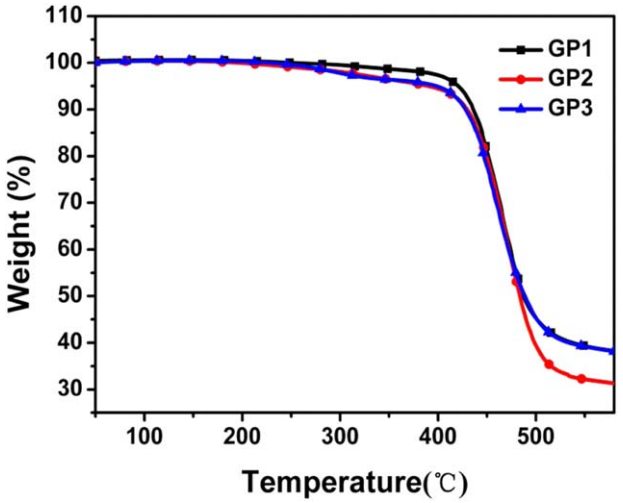


**Figure 2.** TGA curves of the terpolymers with a scan rate of 20°C $min^{-1}$ under nitrogen atmosphere. [Color figure can be viewed in the online issue, which is available at wileyonlinelibrary.com.]

the other absorption bands at longer wavelengths (550–900 nm) with the $\lambda_{s,\ max}$ at 644 nm, 644 nm, and 671 nm, respectively, are attributed to ICT between the TBT and DPP units. It can be seen that the absorption peak of **GP3** has red-shifted compared with **GP1** and **GP2**, because **GP3** has not side gourp on thiophene ($R_2 = H$) which make the ICT more obvious. Compared with the absorption spectra in the solution, the maximum absorption peaks ($\lambda_{f,max}$) of terpolymers **GP1, GP2,** and **GP3** in solid films are red-shifted about 75, 94, and 59 nm, respectively. This can be explained as the low interaction between the polymer chains in solution due to chain length and branching. The terpolymer **GP2** showed a maximum red-shift (94 nm) due to linear chain both R1 and R2 resulting in stronger interaction between the polymer chains. Furthermore, It is noticed that the terpolymers in film show a strong shoulder peak (657–738 nm), suggesting more orderly $\pi-\pi$ stacking in the solid state.[35] According to the absorption spectra of the films [Figure 3(b)], the optical gaps of the terpolymers, deduced from their absorption edges, are 1.57 eV for **GP1**, 1.55 eV for **GP2**, and 1.55 eV for **GP3,** respectively, both near ideal optical gaps (1.1–1.5 eV).[36]

### Electrochemical Properties

The cyclic voltammetry (CV) was employed to examine the electrochemical properties and evaluate the HOMO and LUMO energy levels of the polymers. The CV curves were recorded by using Pt plate as working electrode, Ag/AgCl (Ag in saturated KCl solution) electrode as a reference and Pt wire as a counter electrode. Figure 4 shows the CV curves of the polymers and ferrocene, and their electrochemical data are listed in Table II. The potentials were referenced to the ferrocene/ferrocenium redox couple (Fc/Fc+). The redoxpotential of Fc/Fc+ was

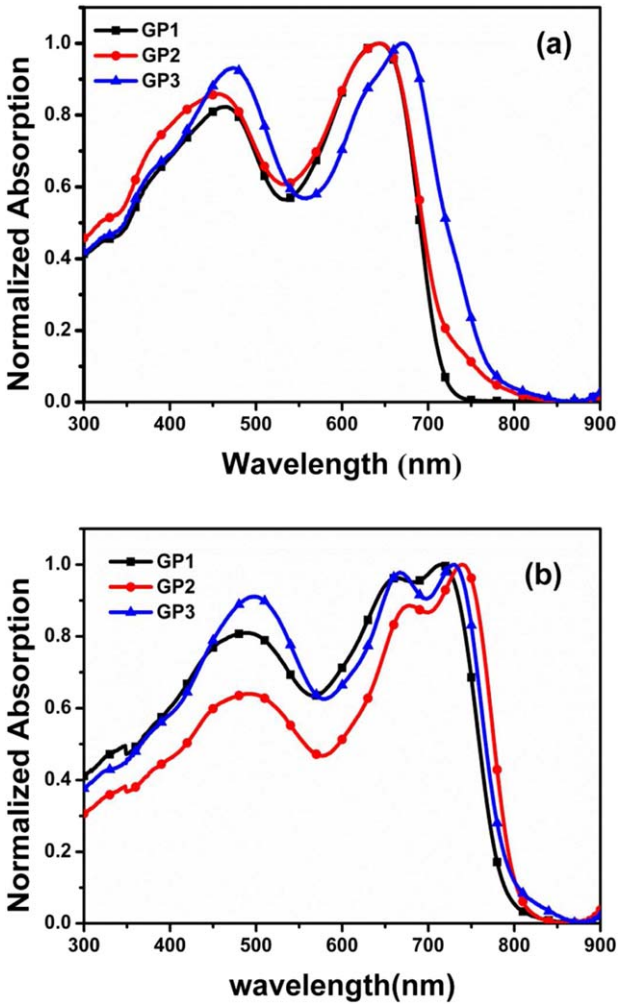


**Figure 3.** UV-Vis-NIR absorption of the terpolymers in the $CHCl_3$ solution (a) and thin films (b). [Color figure can be viewed in the online issue, which is available at wileyonlinelibrary.com.]

**Table II.** Photophysical and Electrochemical Properties of the Terpolymers

| Polymers | Solution $\lambda_{s,max}$ (nm)[a] Abs. | Film $\lambda_{f,max}$ (nm) Abs. | Film $\lambda_{edge}$ (nm) Abs. | $E_g^{opt}$ (eV)[b] | HOMO (eV)[c] | LUMO (eV)[d] |
|---|---|---|---|---|---|---|
| GP1 | 644 | 718 | 791 | 1.57 | −5.29 | −3.72 |
| GP2 | 644 | 726 | 801 | 1.55 | −5.16 | −3.61 |
| GP3 | 671 | 741 | 792 | 1.57 | −5.17 | −3.60 |

[a] Measured in chloroform solution.
[b] Band gap estimated from the optical absorption band edge of the films.
[c] HOMO energy levels measured from cyclic voltammetry.
[d] Calculated from the optical band gaps and HOMO energy.

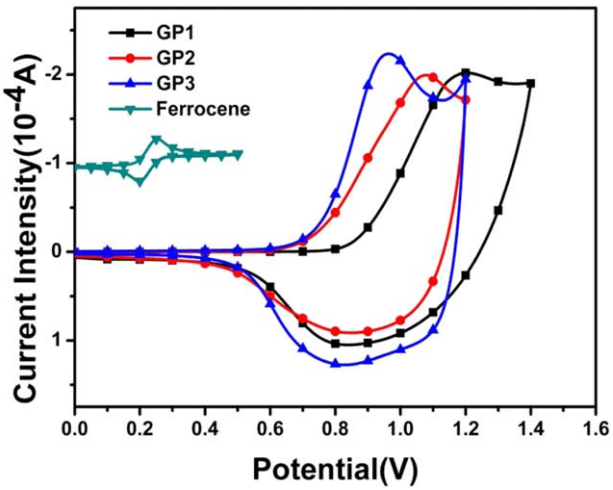


**Figure 4.** Cyclic voltammograms of the terpolymer films on a platinum electrode in 0.1 mol $L^{-1}$ $Bu_4NPF_6$ acetonitrile solution. [Color figure can be viewed in the online issue, which is available at wileyonlinelibrary.com.]

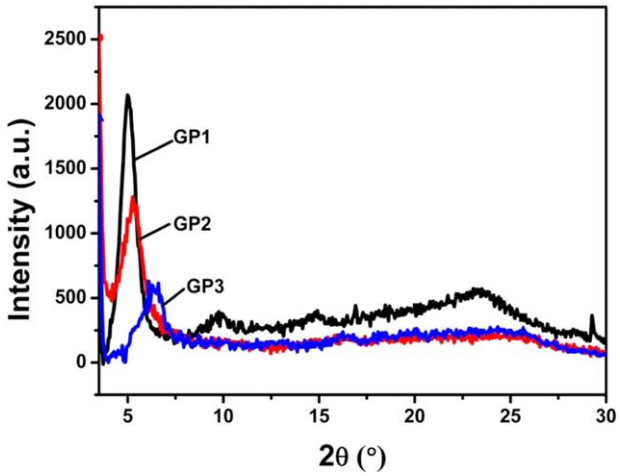


**Figure 5.** WAXRD analysis of the terpolymer films. [Color figure can be viewed in the online issue, which is available at wileyonlinelibrary.com.]

assumed to have an absolute energy level of −4.8 eV under vacuum,[37] it has been measured under the same conditions as the polymer samples and was located at 0.38 V related to the $Ag/Ag^+$ electrode. The onset potentials for oxidation ($E_{ox}$) are observed to be 0.87, 0.74 and 0.75 V for **GP1**, **GP2** and **GP3**, respectively. The HOMO energy levels of the terpolymers were calculated according to the equation: HOMO = −e ($E_{ox}$ + 4.42) eV, so the HOMO energy levels were −5.29 eV, −5.16 eV and −5.17 eV for **GP1**, **GP2** and **GP3** respectively. The polymers with all branched alkyl chains tend to have slightly deeper HOMO energy levels than those with linear and short alkyl chains. Compared with thiophene, 3-hexylthiophene has higher ionization potential, and ethylhexyl has higher ionization potential than octyl, so the electron densities are lower for 3-hexylthiophene and ethylhexyl. Thus, **GP1** has the lowest HOMO energy level, this indicates that the steric hindrance of bulkier side chains disrupts conjugation along the polymer backbone, slightly weakening the electron-donating effect. In addition, the deep HOMO levels of the three terpolymers are under −5.10 eV indicating good chemical stability in ambient conditions. The LUMO energy levels of **GP1**, **GP2** and **GP3** were −3.72 eV, −3.61 eV, and −3.60 eV calculated from the optical band gaps and HOMO energy levels of the terpolymers.[13]

### X-ray Diffraction

To investigate the effect of the chemical structure on the molecular aggregation of the terpolymers, wide angle X-ray diffraction (WAXRD) of the terpolymer thin films was performed in reflection geometry at 40 mA, 40 kV with Cu-Kα radiation. As shown in Figure 5, every terpolymer exhibits two distinct diffraction peak, a narrow one in the small angle region of 5–6° and another broad one in the large angle range between 15 and 25°. The former band (the 100 peaks) was assigned to the ordered assembly along the molecular arms, the latter one (the 010 peaks) was contributed from the ordered π−π stacking between the conjugated main backbones.[38,39] The WAXRD clearly shows the 100 peaks at 4.99° for **GP1**, 5.21° for **GP2**, 6.07° for **GP3**, corresponding to the lamellar distances of 17.71 Å, 16.96 Å, and 14.56 Å, respectively, **GP3** has the shortest lamellar distances, which resulted in fairly well-ordered crystalline lamellar structures. Simultaneously, the 010 peaks are observed at 23.28° for **GP1**, 24.72° for **GP2**, and 24.28° for **GP3**, indicating the π−π stacking distances of 3.82 Å, 3.60Å and 3.66 Å, respectively. The straighter and shorter aliphatic groups of **GP2** and **GP3**, lead the increased inter- or intramolecular interactions and more clear π−π stacking, and the polymer chains arranged more orderly and more closely resulting in them have smaller lamellar distances. To the contrary, two bulky branched alkyl chains diminished the efficiency of π−π overlap between neighboring polymer backbones which make **GP1** has the largest lamellar distances. The smaller lamellar distances and π−π stacking distances indicate that **GP2** and **GP3** have larger vander Waals force and stronger π−π interaction of the polymer backbone compared with **GP1**. Therefore, **GP2** and **GP3** are expected to possess higher mobility than **GP1**, the hole mobility of these terpolymers was measured using the space charge limited current (SCLC), and the devices were fabricated with the configuration of ITO/PEDOT:PSS (25 nm)/polymer:$PC_{61}BM$/$MoO_3$(20 nm)/Al (100 nm). As expected, **GP2** ($3.29 \times 10^{-4}$ $cm^2$ $V^{-1}$ $s^{-1}$) and **GP3** ($1.46 \times 10^{-4}$ $cm^2$ $V^{-1}$ $s^{-1}$) have higher hole mobility than **GP1** ($2.69 \times 10^{-5}$ $cm^2$ $V^{-1}$ $s^{-1}$). Usually, the random terpolymer possesses a low crystallinity because of varying chemical structures and different unit strengths. However, all of these terpolymers still have a considerable crystallinity because of the highly fused conjugated structure of DPP.

### Film Morphology

To understand the effect of morphology of photoactive layer to the efficiencies of PSCs, the morphologies of the polymers/$PC_{61}BM$ (1/1.5, w/w) blend films were investigated by atomic force microscopy (AFM). As shown in Figure 6, the **GP1** blend film forms nearly invisible phase separation and small surface root mean square roughness (RMS, 0.54 nm), which is due to

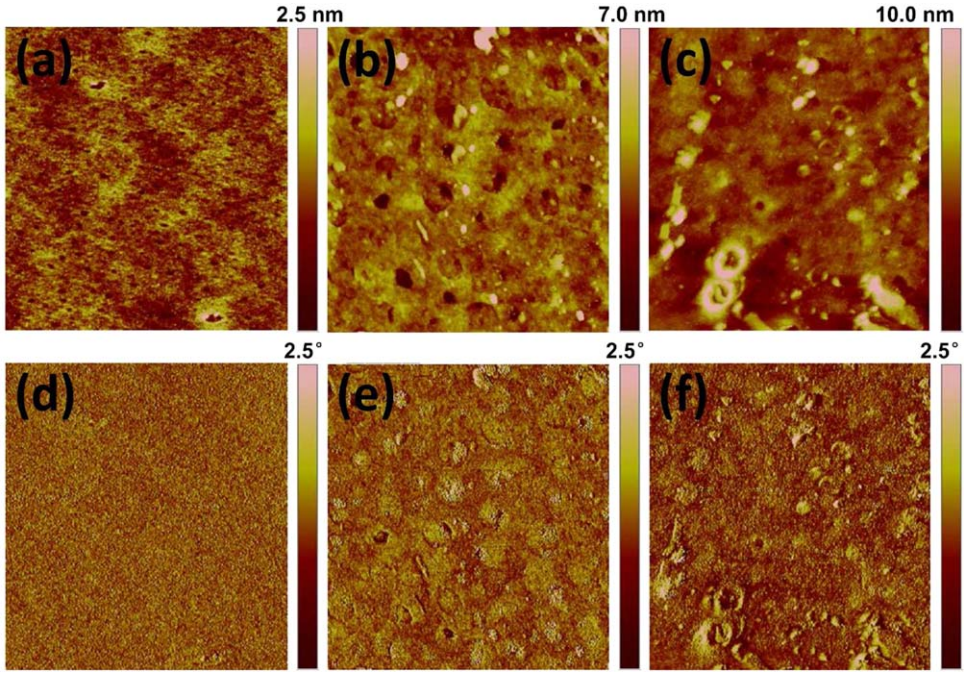


**Figure 6.** AFM height images and phase images (tapping-mode, 3 × 3 $\mu$m) for the terpolymers: $PC_{61}BM$ blend films (w/w 1:1.5). (a) and (d): **GP1**, (b) and (e): **GP2**, (c) and (f): **GP3**. [Color figure can be viewed in the online issue, which is available at wileyonlinelibrary.com.]

**GP1** has longest and bulky aliphatic groups, thus lead to the good miscibility with $PC_{61}BM$. Compared with the **GP1** blend film, the **GP2** and **GP3** blend films possess obvious microphase separation and higher RMS values (1.47 nm for **GP2**, 2.00 nm for **GP3**). Obviously, the size of the branched alkyl chains is critically important in enabling a well-controllable aggregation behaviour. Unnecessarily long alkyl chains cause several detrimental effects including weaker laminar stacking and poorer absorption properties. By modifying the alkyl side chains, the appropriate microphase separation can be obtained. For crystalline polymer the appropriate microphase separation and smaller domain size are beneficial to more effective exciton dissociation and charge transport, so **GP2**/$PC_{61}BM$ blend film would may obtain a better photovoltaic performances.

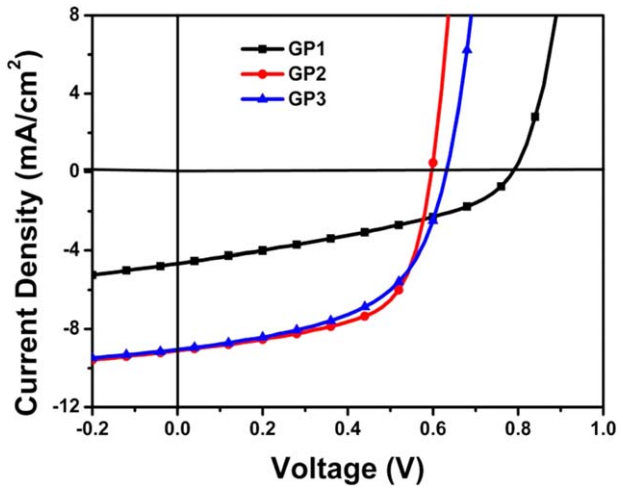


**Figure 7.** J-*V* curves of the PSCs based on the terpolymers under the illumination of AM 1.5 G, 100 mW $cm^{-2}$. [Color figure can be viewed in the online issue, which is available at wileyonlinelibrary.com.]

### Photovoltaic Properties

In order to check the influence of alkyl side chains on photovoltaic performance in the PSCs, the bulk heterojunction PSCs were fabricated with a device structure of ITO/$MoO_3$ (20 nm)/polymer: $PC_{61}BM$/LiF(0.5 nm)/Al(100 nm). The active layers were spin-coated from chlorobenzene. Figure 7 shows the best *J–V* curves of the devices under the illumination of 100 mW/$cm^2$ at AM 1.5 G, and the corresponding photovoltaic parameters including the short-circuit current density ($J_{sc}$), the open-circuit voltage ($V_{oc}$), the fill factor (FF), and power conversion efficiency (PCE), are summarized in Table III.

As is show in Table III, the PSC devices achieved the PCE values of 1.41% for **GP1**, 3.31% for **GP2**, and 3.05% for **GP3**. The sequence of the PCE values for the three terpolymers is according with their absorption spectra, $V_{oc}$ values and the extent of phase separation. As we expected, the PSC device based on **GP1** shows the highest open circuit voltages ($V_{oc}$) of 0.79 V since it

**Table III.** Photovoltaic Properties and Hole Mobility of the Terpolymers

| Polymers/ $PC_{61}BM$ (1 : 1.5, w/w) | $J_{sc}$ (mA $cm^{-2}$) | $V_{oc}$ (V) | FF | PCE (%) | Hole mobility ($cm^2$ $V^{-1}$ $s^{-1}$) |
|---|---|---|---|---|---|
| GP1 | 4.66 | 0.79 | 0.38 | 1.41 | $2.69 \times 10^{-5}$ |
| GP2 | 9.11 | 0.60 | 0.61 | 3.31 | $3.29 \times 10^{-4}$ |
| GP3 | 9.05 | 0.63 | 0.53 | 3.05 | $1.46 \times 10^{-4}$ |

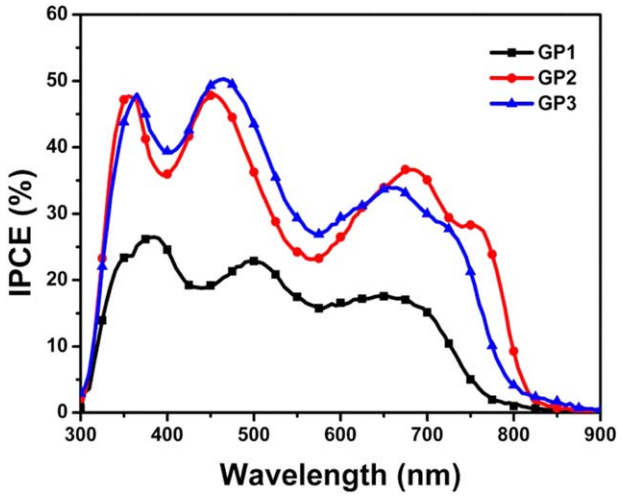


**Figure 8.** IPCE curves of the PSCs based on the terpolymers. [Color figure can be viewed in the online issue, which is available at wileyonlinelibrary.com.]

possess the lowest HOMO energy level, and the device based on **GP2** and **GP3** show lower $V_{oc}$ values of 0.60 V and 0.63 V, respectively. But the **GP1** has the lowest hole mobility of $2.69 \times 10^{-5}$ $cm^2$ $V^{-1}$ $s^{-1}$ which leads to the lowest $J_{sc}$ value of 4.66 mA $cm^{-2}$. However, the **GP2** and **GP3** possess smaller lamellar distance and $\pi-\pi$ stacking distance, so they show the higher hole mobilities of $3.29 \times 10^{-4}$ $cm^2$ $V^{-1}$ $s^{-1}$, $1.46 \times 10^{-4}$ $cm^2$ $V^{-1}$ $s^{-1}$ and the higher $J_{sc}$ values of 9.11 mA $cm^{-2}$ and 9.05 mA $cm^{-2}$.

Meanwhile, PSCs based on the as-synthesized polymers blended with $PC_{61}BM$ were tested for their incident photon-to-current conversion efficiencies (IPCE). Typical curves are shown in Figure 8. The GP1 device only shows a low IPCE response between 300 and 750 nm with a maximum IPCE value of only 26.41% at 380 nm, which corresponds to the minimum hole mobility. However, the **GP2** and **GP3** device exhibit broader and uniform IPCE responses over 300–800 nm with a maximum IPCE value of 50.29% at 465 nm and 47.84% at 450 nm. Obviously, GP2 shows the highest IPCE among them, which is in line with the $J_{sc}$ form these value, we can found that the IPCE could be improved via the modification of alkyl side chains.

## CONCLUSIONS

In summary, three novel random conjugated terpolymers based on DPP and DTBT side groups have been synthesized and characterized. The random terpolymers appear promising for the application in BHJ solar cells due to their wide spectrum and low energy band-gap, and the optical and electrochemical properties of the terpolymers were optimized by tuning the alkyl side chain. We found that the terpolymer **GP1** with long and bulky alkyl side chain shows a deeper HOMO energy level of −5.29 eV. However, the PSC device based on **GP1** exhibits a low $J_{sc}$ and PCE because of its largest lamellar distance and $\pi-\pi$ stacking distance. The polymer **GP3** shows smaller lamellar distance and $\pi-\pi$ stacking distance, but its domain size is larger relatively, so the PSC device based on **GP3** has the medium $J_{sc}$ and PCE. **GP2** has an appropriate alkyl side chain, so it possesses more orderly $\pi-\pi$ stacking and broader absorption range and the appropriate microphase separation, which leads to higher $J_{sc}$ of 9.11 mA/$cm^2$ and PCE of 3.31%.

## ACKNOWLEDGMENTS

This work was supported by the National Natural Science Foundation of China (21474081), and Hunan Provincial Natural Science Foundation of China (13JJ2025, 2015JJ2141).

## REFERENCES

1. Liu, Y.; Zhao, J.; Li, Z.; Mu, C.; Ma, W.; Hu, H.; Jiang, K.; Lin, H.; Ade, H.; Yan, H. *Nat. Commun.* **2014**, *5*, 5293.
2. Chen, J.-D.; Cui, C. H.; Li, Y.-Q.; Zhou, L.; Ou, Q.-D.; Li, C.; Li, Y. F.; Tang, J.-X. *Adv. Mater.* **2015**, *27*, 1035.
3. Nielsen, C. B.; Ashraf, R. S.; Schroeder, B. C.; D'Angelo, P.; Watkins, S. E.; Song, K.; Anthopoulos, T. D.; McCulloch, I. *Chem. Commun.* **2012**, *48*, 5832.
4. Han, L.; Chen, W.; Hu, T.; Ren, J.; Qiu, M.; Zhou, Y.; Zhu, D.; Wang, N.; Sun, M.; Yang, R. *ACS Macro Lett.* **2015**, *4*, 361.
5. Chan, W.-L.; Ligges, M.; Jailaubekov, A.; Kaake, L.; Miaja-Avila, L.; Zhu, X. Y. *Science* **2011**, *334*, 1541.
6. Chen, H. C.; Chen, Y. H.; Liu, C. C.; Chen, Y. C.; Chou, S. W.; Chou, P. T. *Chem. Mater.* **2012**, *24*, 4766.
7. Qin, R. P.; Jiang, Y. R.; Zhang, K. X.; Zhang, H. X.; Zhang, Q. Y.; Li, M.; Ma, H. *J Appl. Polym. Sci.* **2015**, *132*, 41587.
8. Zhang, J. Q.; Zhang, Y. J.; Fang, J.; Lu, K.; Wang, Z. Y.; Ma, W.; Wei, Z. X. *J Am. Chem. Soc.* **2015**, *137*, 8176.
9. Liu, S.; Bao, X. C.; Li, W.; Wu, K. L.; Xie, G. H.; Yang, R. Q.; Yang, C. L. *Macromolecules* **2015**, *48*, 2948.
10. Zhang, F. J.; Xu, X. W.; Tang, W. H.; Zhang, J.; Zhuo, Z. L.; Wang, J.; Xu, Z.; Wang, Y. S. *Sol. Energy Mater. Sol. Cells* **2011**, *95*, 1785.
11. Zhang, M. J.; Gu, Y.; Guo, X.; Liu, F.; Zhang, S. Q.; Huo, L. J.; Russell, T. P.; Hou, J. H. *Adv. Mater.* **2013**, *25*, 4944.
12. Li, H. H.; Luo, H.; Cao, Z.; Gu, Z. J.; Shen, T. P.; Zhao, B.; Chen, H. J.; Yu, G.; Tan, S. T. *J Mater. Chem.* **2012**, *22*, 22913.
13. Hu, X.; Zuo, L.; Fu, W.; Larsen-Olsen, T. T.; Helgesen, M.; Bundgaard, E.; Hagemann, O.; Shi, M.; Krebs, F. C.; Chen, H. *J J. Mater. Chem.* **2012**, *22*, 15710.
14. Wang, E.; Hou, L.; Wang, Z.; Hellstrom, S.; Zhang, F.; Inganas, O.; Andersson, M. R. *Adv. Mater.* **2010**, *22*, 5240.
15. Jung, J. W.; Liu, F.; Russell, T. P.; Jo, W. H. *Energy Environ. Sci.* **2013**, *6*, 3301.
16. Kim, H. G.; Kang, B.; Ko, H.; Lee, J.; Shin, J.; Cho, K. *Chem. Mater.* **2015**, *27*, 829.
17. Li, J.; Ong, K. H.; Sonar, P.; Lim, S. L.; Ng, G. M.; Wong, H. K.; Tan, H. S.; Chen, Z. K. *Polym. Chem.* **2013**, *4*, 804.
18. Hou, Q.; Liu, J. G.; Jia, T.; Luo, S. L.; Shi, G. *J Appl. Polym. Sci.* **2013**, *130*, 3276.

19. Meager, I.; Ashraf, R. S.; Rossbauer, S.; Bronstein, H.; Donaghey, J. E.; Marshall, J.; Schroeder, B. C.; Heeney, M.; Anthopoulos, T. D.; McCulloch, I. *Macromolecules* **2013**, *46*, 5961.
20. Kang, T. E.; Cho, H.-H.; Kim, H.; Lee, W.; Kang, H.; Kim, B. *J Macromolecules* **2013**, *46*, 6806.
21. Shin, J.; Park, G. E.; Lee, D. H.; Um, H. A.; Lee, T. W.; Cho, M. J.; Choi, D. H. *ACS Appl. Mater. Interfaces* **2015**, *7*, 3280.
22. Bronstein, H.; Chen, M. Z.; Ashraf, R. S.; Zhang, W.; Du, J.; Durrant, J. R.; Tuladhar, P. S.; Song, K.; Watkins, S. E.; Geerts, Y.; Wienk, M. M.; Janssen, R. A.; Anthopoulos, T.; Sirringhaus, H.; Heeney, M.; McCulloch, I. *J Am. Chem. Soc.* **2011**, *133*, 3272.
23. Dou, L.; Chang, W. H.; Gao, J.; Chen, C. C.; You, J. B.; Yang, Y. *Adv. Mater.* **2013**, *25*, 825.
24. Jung, J. W.; Liu, F.; Russell, T. P.; Jo, W. H. *Energy Environ. Sci.* **2012**, *5*, 6857.
25. Li, W. W.; Hendriks, K. H.; Furlan, A.; Wienk, M.; Janssen, R. *J Am. Chem. Soc.* **2015**, *137*, 2231.
26. Nielsen, C. B.; Turbiez, M.; McCulloch, I. *Adv. Mater.* **2013**, *25*, 1859.
27. Ye, L.; Zhang, S.; Ma, W.; Fan, B.; Guo, X.; Huang, Y.; Ade, H.; Hou, J. *Adv. Mater.* **2012**, *24*, 6335.
28. Yiu, A. T.; Beaujuge, P. M.; Lee, O. P.; Woo, C. H.; Toney, M. F.; Frechet, J. M. *J. Am. Chem. Soc.* **2012**, *134*, 2180.
29. Gu, Z. J.; Shen, P.; Tsang, S.-W.; Tao, Y.; Zhao, B.; Tang, P.; Nie, Y.; Fang, Y.; Tan, S. T. *Chem. Commun.* **2011**, *47*, 9381.
30. Hou, R. Y.; Zhao, B.; Wu, F.; Wang, G.; Shen, T. P.; Guo, H.; Zhang, J.; Chen, H. J.; Tan, S. T. *Organ. Electron.* **2015**, *20*, 142.
31. Livi, F.; Zawacka, N.; Angmo, D.; Jorgensen, M.; Krebs, F.; Bundgaard, E. *Macromolecules* **2015**, *48*, 3481.
32. Lee, J. Y.; Jo, J. W.; Jo, W. H. *Organic Electronics* **2015**, *02*, 1566.
33. Bronstein, H.; Hurhangee, M.; Fregoso, E. C.; Beatrup, D.; Soon, Y. W.; Huang, Z.; Hadipour, A. *Chem. Mater.* **2013**, *25*, 4239.
34. Jen, T. H.; Huang, S. P.; Chen, Y.-C.; Hsiao, A.-E.; Yin, S.-H.; Chen, H.-Y.; Chen, S.-A. *J. Am. Chem. Soc.* **2008**, *03*, 13.
35. Sato, T.; Kokubo, H.; Yamamoto, T.; *Macromolecules* **2009**, *39*, 3
36. He, Z.; Xiao, B.; Liu, F.; Wu, H.; Yang, Y.; Xiao, S.; Wang, C.; Russell, T. P.; Cao, Y. *Nat. Photo.* **2015**, *5*, 174.
37. Li, Y.; Cao, Y.; Gao, J.; Wang, D.; Yu, G.; Heeger, A. *J. Synth. Met.* **1999**, *99*, 243.
38. Dutta, P.; Yang, W.; Lee, W. H.; Kang, N.; Lee, S. H. *J. Mater. Chem.* **2012**, *22*, 10840.
39. Liu, Y.; Wan, X.; Wang, F.; Zhou, J.; Long, G.; Tian, J.; You, J.; Yang, Y.; Chen, Y. *Adv. Energy Mater.* **2011**, *1*, 771.